Balakrishnan et al.

Molecular Profiling of the 'Plexinome' in melanoma and pancreatic cancer

SUPPORTING INFORMATION

SUPP. METHODS

Copy number analysis

Quantitative real-time TaqMan PCR was performed to determine copy number of all the plexins in melanoma and PDAC tumors. Target sequences were designed for all nine plexins and the respective Custom TaqMan® Assays were ordered from Applied Biosystems (Applied Biosystems, Foster City, CA). Two assays were designed and ordered for *PLXNA4*. The probes were labeled with the reporter dye 6-carboxyfluorescein (FAM) and Non-fluorescent quencher (NFQ), at the 5'- and 3'- ends, respectively. PCR was performed in a 384-well clear optical reaction plate using the ABI Prism 7900HT Sequence detection system (Applied Biosystems, Foster City, CA). All reactions were performed in triplicate. The average *PLXN* copy number was calculated from the differences in the threshold amplification cycles between *PLXN* and RNaseP. The diploid retinal pigmental epithelial cell line (RPE) was used as a normal control. Copy number was determined from the PCR cycle number (Ct) at which the fluorescence from the DNA reaches a threshold amount of fluorescence above the background. Calculations were performed according to the δδCt method (Livak et al., 2001). The Ct values for each set of triplicates were averaged. The Ct of the reference was subtracted from the Ct for each locus to obtain the δCt [δCt = Ct (plexin) - Ct (RNaseP)]. δCt values were determined for loci in tumor samples and normal diploid genomic DNA (RPE). The relative copy number of a locus is tumor DNA to normal DNA = $2^{-\delta\delta Ct}$, where δδCt = δCt (tumor) -δCt (normal). Copy numbers <1.5, 1.5 to 3.0, and >3.0 copies per sample were cutoff values to indicate decreased, normal, and increased *PLXN* copy numbers respectively (Takano et al., 2005).

Ectopic expression of plexins in mammalian cells

cDNAs encoding human plexins were modified by site directed mutagenesis (Quickchange II XL kit, Stratagene) to introduce the nucleotide mutations identified in human tumors. The R539H mutation was introduced in a construct encoding the extracellular and transmembrane domain of human-PLXNB3, to be used for binding assays. The p.H1736Y mutation of PLXNA4 was introduced in a construct expressing the transmembrane and cytoplasmic domain of the human receptor, to be used for testing the cell collapsing activity. The latter construct was designed by analogy to the constitutively active constructs previously generated for PLXNA1 and PLXNB1 (Takahashi et al., 2001; Oinuma et al., 2004) and included the coding sequence starting from amino acid residue Alanine at 1214. The p.E1154K mutation of PLXNA4 was introduced in a construct encoding full size mouse receptor (as the human complete cDNA was not available), and mouse secreted Sema6A-AP (kindly provided by H. Fujisawa, Japan) was used as probe in binding assays (see below). Ectopic expression of wild type or mutated plexins in COS and MDA-MB435 cells was achieved by DNA transfection. Protein expression was assessed by immunoblotting, according to standard methods. Anti-VSV-G and anti-Myc-tag antibodies were from Sigma.

Functional assays to analyze mutated plexins

Semaphorin binding assays were performed as previously described (Tamagnone et al., 1999). Briefly, COS cells transfected to express plexin constructs were incubated with 2nM recombinant secreted Sema5A fused to alkaline-phosphatase (Sema5A-AP)(Artigiani et al., 2004). Cell-bound semaphorin was eventually revealed by incubating with NBT/BCIP alkaline phosphatase substrate (Promega).

Cellular collapse assays were performed as previously described (Barberis et al., 2004). Briefly, COS cells transfected to express constitutively active plexin constructs were seeded on fibronectin-coated glass coverslips and subjected to immunofluorescence analysis. F-actin was stained with fluorescein-labeled phalloidin (phalloidin-FITC, Sigma) to provide counterstaining. Digital images were acquired, using a Zeiss Axyoskop microscope equipped with Biorad Confocal Imaging System. Collapsed cells were identified for having a diameter equal or less than 30 μm.

Cell migration assays were performed as previously described (Barberis et al., 2004). Briefly, the lower side of the semipermeable membrane of Transwell inserts (Costar) was previously coated with 10ug/ml fibronectin (Sigma). 1x10e5 MDA-MB435 cells were then seeded in the upper chamber of the insert and let spontaneously migrate through the pores of the membrane for 16 hours. The migrated cells found on the lower side of the filter were fixed, stained with crystal violet, photographed and counted using Metamorph software.

SUPP. TABLES:

Supp. Table S1. A summary of information on the nine known human plexins.

Gene	Gene Symbol	Synonyms/Description	No. Exons	Chromosome
PLEXIN A1	*PLXNA1*	Plexin-A1 precursor (Semaphorin receptor NOV), NOVP, PLEXIN-A1, PLXN1	31	3q21.3
PLEXIN A2	*PLXNA2*	RP11-328D5.3, FLJ11751, FLJ30634, KIAA0463, OCT, PLXN2	32	1q32.2
PLEXIN A3	*PLXNA3*	XX-FW81657B9.3, 6.3, HSSEXGENE, PLEXIN-A3, PLXN3, PLXN4, SEX, XAP-6	33	Xq28
PLEXIN A4	*PLXNA4*	DKFZp566O0546, FLJ35026, FLJ38287, PLEXA4, PLXNA4	31	7q32.3
		DKFZp434G0625, DKFZp434G0625PRO34003, FAYV2820, PRO34003	5	
PLEXIN B1	*PLXNB1*	KIAA0407, PLEXIN-B1, PLXN5, SEP	36	3p21.31
PLEXIN B2	*PLXNB2*	KIAA0315, MM1, Nbla00445, PLEXB2, dJ402G11.3	35	22q13.33
PLEXIN B3	*PLXNB3*	PLEXB3, PLEXR, PLXN6	36	Xq28
PLEXIN C1	*PLXNC1*	CD232, PLXN-C1, VESPR (Virus Encoded Semaphorin Protein Receptor), KIAA0620	31	12q23.3
PLEXIN D1	*PLXND1*	KIAA0620, MGC75353, PLEXD1	37	3q21.3

The total number of exons in each gene and the location of the plexins in the genome are tabulated. *PLXNA4* genomic sequence had been initially reported in public databases as split into two records corresponding to adjacent loci (*PLXNA4-A* and *PLXNA4-B*).

Supp. Table S2. Information on tumor samples.

Tumor type	Sample	Age	Gender	Grade	Tumor source	Tumor DNA source	Matched Normal source
Melanoma	2A	51	M	IV	nodal metastasis	short term cultures	EBV immortalized B lymphocytes
	4A	55	F	IIB/IIIC	primary tumour	short term cultures	EBV immortalized B lymphocytes
	5A	36	F	IIIB/IIIC	nodal metastasis	short term cultures	EBV immortalized B lymphocytes
	6A	43	M	IIIC	nodal metastasis	short term cultures	EBV immortalized B lymphocytes
	7A	22	F	IIIB/IIIC	nodal metastasis	short term cultures	EBV immortalized B lymphocytes
	8A	55	M	IIIC	nodal metastasis	short term cultures	EBV immortalized B lymphocytes
	9A	53	M	IIIB/IIIC	nodal metastasis	short term cultures	EBV immortalized B lymphocytes
	10A	52	M	IIIC	nodal metastasis	short term cultures	EBV immortalized B lymphocytes
	11A	69	M	IIIA/IIIB	nodal metastasis	short term cultures	EBV immortalized B lymphocytes
	12A	70	M	IV	cutaneous metastasis	short term cultures	EBV immortalized B lymphocytes
	13A	59	F	IV	cutaneous metastasis	short term cultures	EBV immortalized B lymphocytes
	14A	56	M	III	nodal metastasis	short term cultures	EBV immortalized B lymphocytes
	15A	30	M	IV-M1c	colon metastasis	short term cultures	EBV immortalized B lymphocytes
	16A	45	F	IIIB/IIIC	nodal metastasis	short term cultures	EBV immortalized B lymphocytes
	17A	51	M	IV	cutaneous metastasis	short term cultures	EBV immortalized B lymphocytes
	18A	68	M	IV	cutaneous metastasis	short term cultures	blood
	19A	71	F	IIIC T4aN3M0	cutaneous metastasis	short term cultures	EBV immortalized B lymphocytes
	20A	24	M	IIIC	nodal metastasis	short term cultures	EBV immortalized B lymphocytes
	21A	36	F	IIIB/IIIC	nodal metastasis	short term cultures	EBV immortalized B lymphocytes
	22A	39	F	IIIC	nodal metastasis	short term cultures	blood
	23A	56	M	IV-M1c	lung metastasis	short term cultures	EBV immortalized B lymphocytes
	24A	49	M	IV	cutaneous metastasis	short term cultures	EBV immortalized B lymphocytes
	25A	49	M	IV	cutaneous metastasis	short term cultures	EBV immortalized B lymphocytes
	26A	62	F	IV-M1a	nodal metastasis	short term cultures	EBV immortalized B lymphocytes
Pancreatic Ductal Adenocarcinoma	360	76	F	T3N0/ G2	primary tumour	xenograft	duodenum
	362	54	M	T3N1b/G3	primary tumour	xenograft	pancreas
	369	61	M	T3N0/G2	primary tumour	xenograft	not available
	370	52	F	T3N1b/G2	primary tumour	xenograft	EBV immortalized B lymphocytes
	371	57	M	T3N0/G3	primary tumour	xenograft	duodenum
	374	62	F	T3N0/G3	primary tumour	xenograft	pancreas
	375	59	M	T3N1a/G3	primary tumour	xenograft	EBV immortalized B lymphocytes
	377	52	M	T3N1a/G2	primary tumour	xenograft	pancreas
	379	62	F	T3N1/G2	primary tumour	xenograft	spleen
	380	57	M	T3N1a/G2	primary tumour	xenograft	duodenum
	382	44	F	T3N0/G2	primary tumour	xenograft	duodenum
	384	69	F	T3N0/G2	primary tumour	xenograft	spleen

Clinical information on the patient and the tumor source are indicated. In addition, the method of tumor propagation prior to DNA extraction is indicated as “tumor DNA source”.

Supp. Table S3. Cell line names and types used for copy number determination of *PLXNA4*.

Cell Line	Origin
RPE	Retinal pigmental epithelial
MET5A	normal human mesothelial cells
MCF10A	breast epithelium (immoratlized, not transformed)
MCF7	breast adenocarcinoma
T47D	breast adenocarcinoma
SKBR3 WT	breast adenocarcinoma
Hs 578T	breast ductal carcinoma*
HCC1008	breast carcinoma*
HCC1954	breast ductal carcinoma*
HCC38	breast ductal carcinoma*
HCC1143	breast ductal carcinoma*
HCC1187	breast ductal carcinoma*
HCC1395	breast ductal carcinoma*
HCC1599	breast ductal carcinoma*
HCC1937	breast ductal carcinoma*
HCC2157	breast ductal carcinoma*
HCC2218	breast ductal carcinoma*
Hs 574.T	breast ductal carcinoma*
MDA MB-231	breast adenocarcinoma
MDA MB-435	melanoma
LOX IMVI	malignant amelanotic melanoma
A431	skin, squamous cell carcinoma
SCC68	squamous cell carcinoma, head and neck
PCI13	squamous cell carcinoma, head and neck
PCI4a	squamous cell carcinoma, head and neck
CAPAN-1	pancreatic adenocarcinoma
BXPC3	pancreatic adenocarcinoma
SUIT-2	pancreatic carcinoma
DIFI WT	colorectal adenocarcinoma
LOVO WT	colorectal adenocarcinoma
HCT116	colorectal adenocarcinoma
HT29	colorectal adenocarcinoma
DLD1	colon carcinoma
SW480	colon adenocarcinoma
U2-WT	osteosarcoma
KHOS	osteosarcoma
SAOS	osteosarcoma
MNNG/HOS	osteosarcoma
MG 63	osteosarcoma
SKNSH	neuroblastoma
LAN-5	neuroblastoma
IMR5	neuroblastoma
TOV21G	ovary, malignant adenocarcinoma
NIH:OVCAR-3	ovarian carcinoma
OV90	ovary, malignant papillary serous adenocarcinoma
PC 3	prostate adenocarcinoma
DU 145	prostate carcinoma

Cell Line	Origin
HEPG2	hepatocellular carcinoma
Hela	cervical adenocarcinoma
U937	leukemic monocyte lymphoma
K562	chronic myelocytic leukemia
GTL16	gastric carcinoma
A549	lung adenocarcinoma
NCI-H1395	lung carcinoma*
NCI-H1437	lung carcinoma*
NCI-H2009	lung carcinoma*
NCI-H2122	lung carcinoma*
NCI-H2087	lung carcinoma*
NCI-H2171	lung carcinoma*
NCI-H2195	lung carcinoma*
NCI-H1184	lung carcinoma*
NCI-H209	lung carcinoma*
NCI-H128	lung carcinoma*
NCI-H2126	lung carcinoma*
NCI-H2107	lung carcinoma*

***** These cell lines were directly obtained from ATCC.

Supp. Table S4, containing sequencing primers, is provided as a separate *.xls file due to its large size.

SUPP. FIGURES:

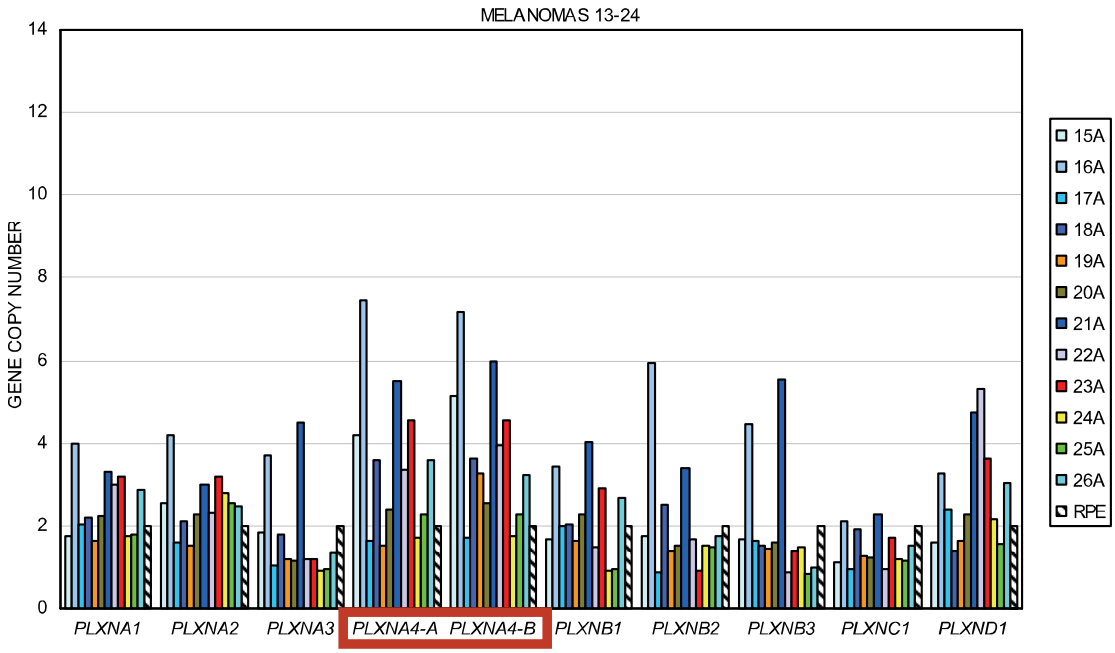

Supp. Figure S1. Plexin gene copy number analysis in melanoma.
Quantitative Real Time PCR analysis with plexin-specific probes of the genomic DNA derived from twelve of the 24 melanomas (the same samples that we sequenced for mutational profiling). Copy number results for the first 12 melanoma samples are shown in Fig.1*A*. The nine plexins are indicated on the X-axis (A1 through D1); two distinct probes were used to analyze *PLXNA4*. The Y-axis shows copy numbers after normalization with control DNA (RPE cells). Gene copy numbers below 1.5 and above 3 are normally considered as aberrant.

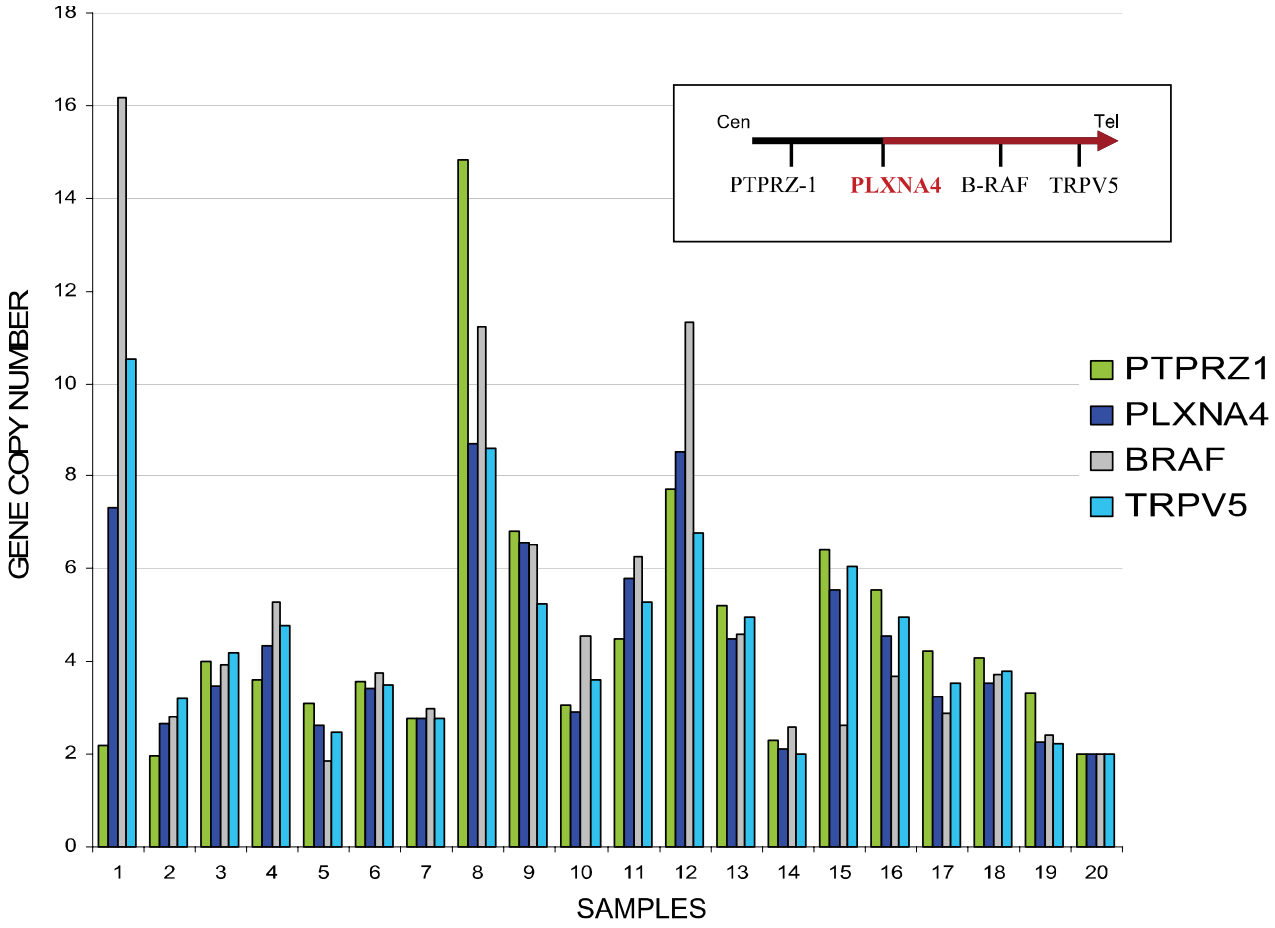

Supp. Figure S2. Delineation of *PLXNA4*-containing amplicon.
To delineate the outermost limits of the *PLXNA4*-containing amplicon in chr. 7q found in melanomas, we determined gene copy numbers of *PLXNA4* along with those of flanking genes *PTPRZ1* and *TRPV5* (located 10Mb upstream and downstream, respectively). In addition, copy number of *BRAF*, located about 8Mb downstream of *PLXNA4*, was also analysed. On the Y-axis, values indicate gene copy numbers, measured by Quantitative Real Time PCR in twenty melanoma samples presenting *PLXNA4* gene amplification (distributed on X-axis).

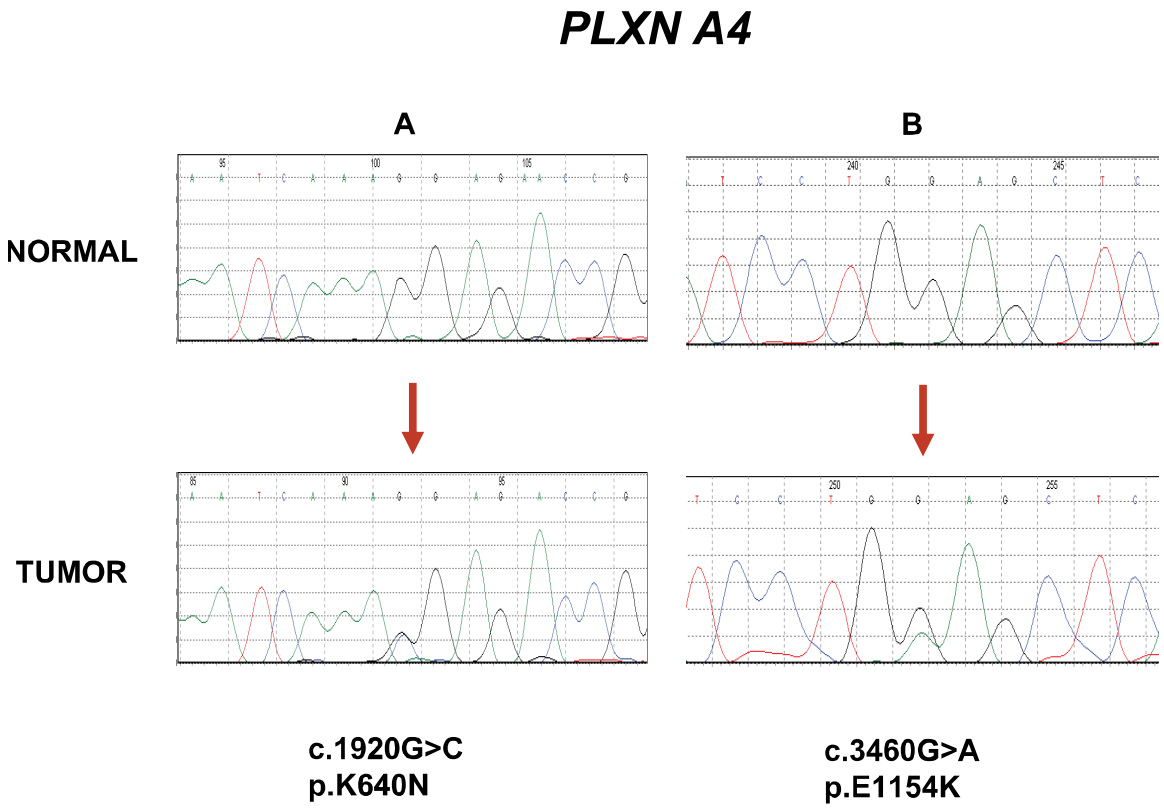

Supp. Figure S3. Somatic mutations in *PLXNA4*.
Chromatograms of the two somatic mutations found in *PLXNA4* in two different melanomas. A third mutation of the same gene, found in a distinct sample is shown in Fig. 2 (main text). In each case, the lower chromatogram belongs to a tumor sample, and the upper chromatogram is from the matched normal. Arrows indicate the location of missense somatic mutations, and the nucleotide and amino acid alterations are indicated below the traces. Numbers above the sequences are part of the software output.

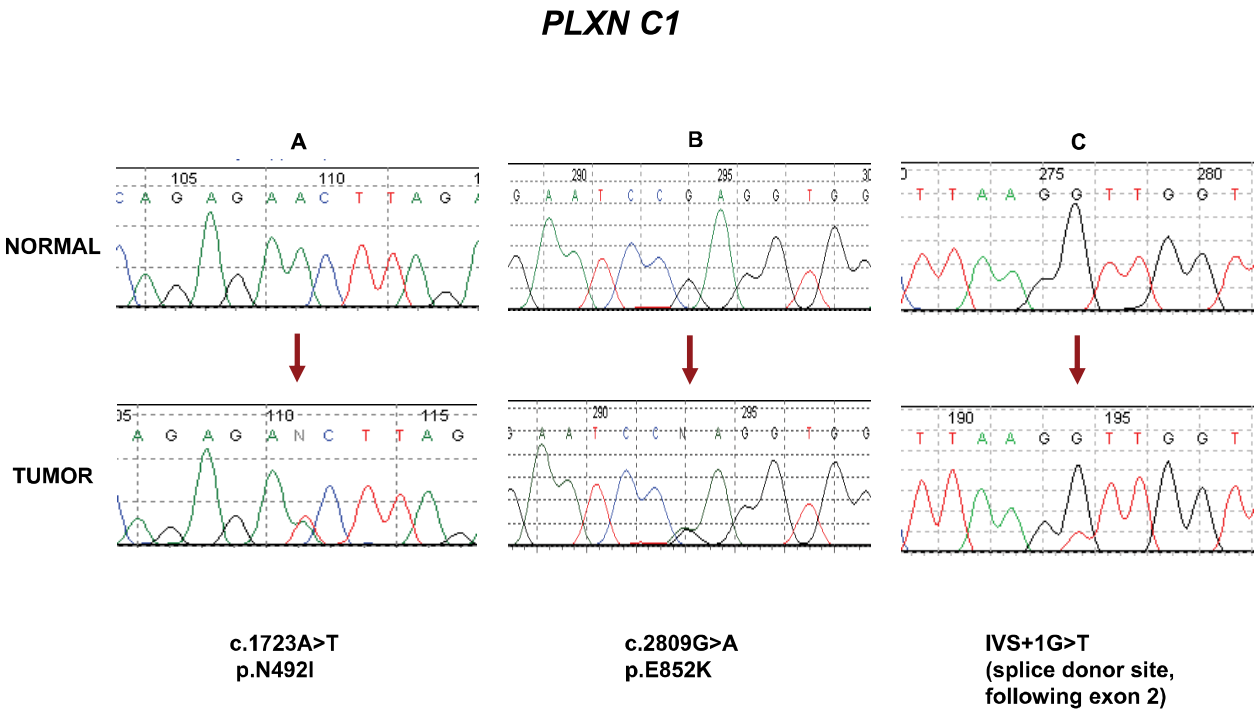

Supp. Figure S4. Somatic mutations in *PLXNC1*.
Chromatograms of the two somatic mutations found in *PLXNC1* in two PDAC samples (A and B). In both, the lower chromatogram belongs to a tumor sample, and the upper chromatogram is from the matched normal. Arrows indicate the location of missense somatic mutations, and the nucleotide and amino acid alterations can be found below each chromatogram pair.

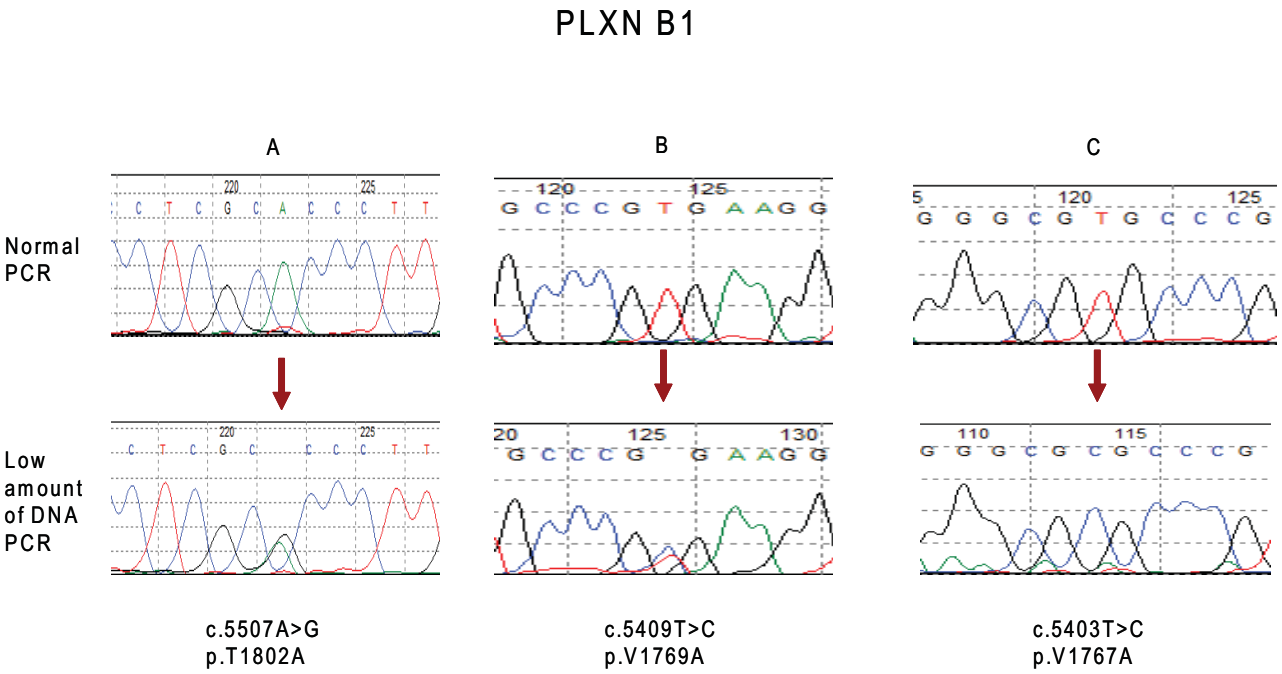

Supp. Figure S5. Direct sequencing of low amounts of DNA may reveal artificial mutations. Chromatograms of three changes (A, B and C) identified in *PLXNB1* in three different prostate cancer samples. In each case, the upper chromatogram belongs to the PCR performed with normal quantity DNA (10ng/10ul reaction), and the lower chromatogram is derived from repeating the same PCR in the same sample but with a lower DNA input (2-5 ng/10ul reaction) showing PCR artifact mutations. p.T1802A mutation is one of those detected by Wong and coworkers (Wong et al., 2004). Arrows indicate the location of the artificial mutations, and the nucleotide and amino acid alterations are indicated below the traces. Numbers above the sequences are part of the software output.

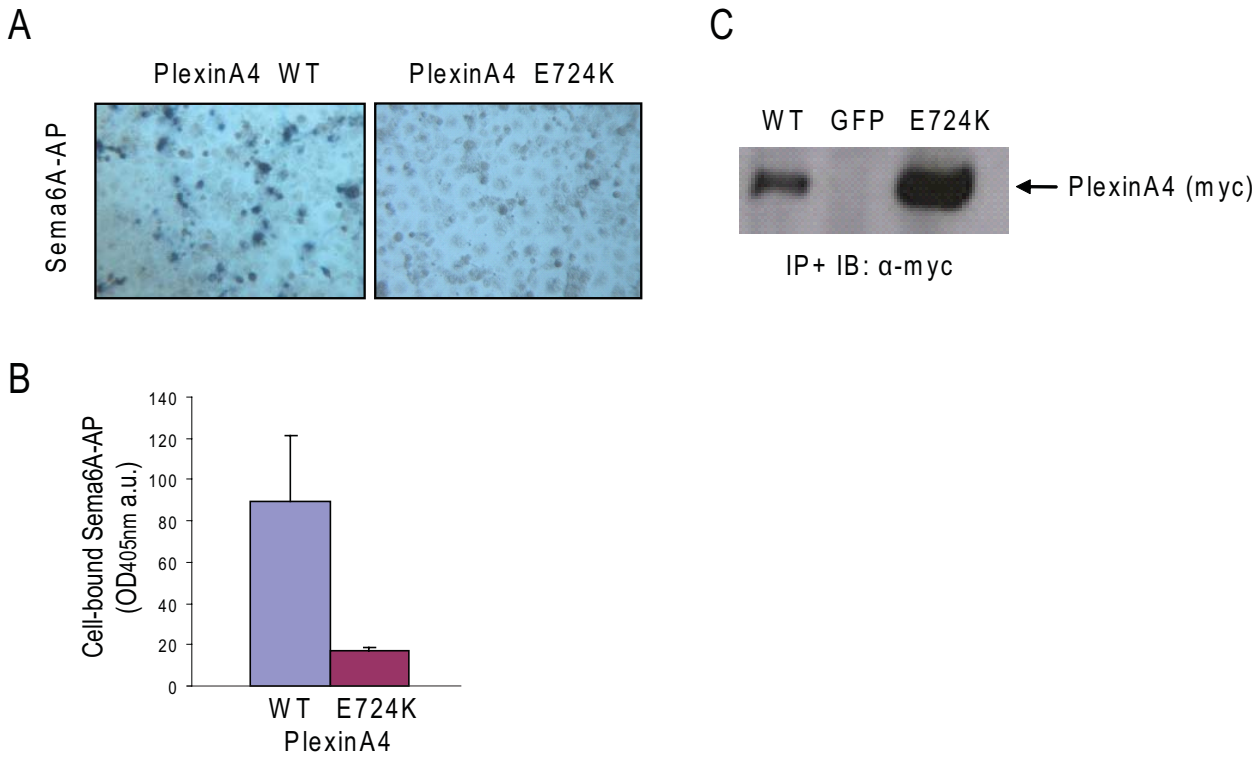

Supp. Figure S6. PLXNA4 p.E1154K mutation impairs ligand binding ability of the receptor.
A, the functional impact of mutation p.E1154K in the extracellular domain of PLXNA4 was assessed in COS cells (see above Methods for details) by challenging the receptor with a soluble form of the specific ligand Sema6A fused to alkaline phosphatase (Sema6A-AP), as previously shown (Suto et al., 2005). Note that, as expected, the ligand also induced a "collapsing" response in cells expressing the WT receptor. B, in order to further quantify ligand binding to receptor-expressing cells, we incubated with the soluble chromogenic AP substrate pNPP, and measured absorbance at 405 nm (see Artigiani et al., 2004 for reference). C, the comparable expression of the WT and mutated receptor proteins in the cells used for the above binding assays was confirmed by Western blotting.

Cited References:

Artigiani S, Conrotto P, Fazzari P, Gilestro GF, Barberis D, Giordano S, Comoglio PM, Tamagnone L. 2004. Plexin-B3 is a functional receptor for semaphorin 5A. EMBO Rep 5:710-714.

Barberis D, Artigiani S, Casazza A, Corso S, Giordano S, Love CA, Jones EY, Comoglio PM, Tamagnone L. 2004. Plexin signaling hampers integrin-based adhesion, leading to Rho-kinase independent cell rounding, and inhibiting lamellipodia extension and cell motility. Faseb J 18:592-594.

Livak KJ and Schmittgen TD. 2001. Analysis of relative gene expression data using real-time quantitative PCR and the 2(-Delta Delta C(T)) Method. Methods 25:402-408.

Oinuma I, Katoh H, Negishi M. 2004. Molecular dissection of the semaphorin 4D receptor plexin-B1-stimulated R-Ras GTPase-activating protein activity and neurite remodeling in hippocampal neurons. J Neurosci 24:11473-11480.

Suto F, Ito K, Uemura M, Shimizu M, Shinkawa Y, Sanbo M, Shinoda T, Tsuboi M, Takashima S, Yagi T, Fujisawa H. 2005. Plexin-A4 mediates axon-repulsive activities of both secreted and transmembrane semaphorins and plays roles in nerve fiber guidance. J Neurosci 25:3628-37.

Takahashi T, Strittmatter SM. 2001. PlexinA1 autoinhibition by the plexin sema domain. Neuron 29:429-439.

Takano T, Ohe Y, Sakamoto H, Tsuta K, Matsuno Y, Tateishi U, Yamamoto S, Nokihara H, Yamamoto N, Sekine I, Kunitoh H, Shibata T, Sakiyama T, Yoshida T, Tamura T. 2005. Epidermal growth factor receptor gene mutations and increased copy numbers predict gefitinib sensitivity in patients with recurrent non-small-cell lung cancer. J Clin Oncol 23:6829-6837.

Tamagnone L, Artigiani S, Chen H, He Z, Ming GI, Song H, Chedotal A, Winberg ML, Goodman CS, Poo M, Tessier-Lavigne M, Comoglio PM. 1999. Plexins are a large family of receptors for transmembrane, secreted, and GPI-anchored semaphorins in vertebrates. Cell 99:71-80.

Wong OG, Nitkunan T, Oinuma I, Zhou C, Blanc V, Brown RS, Bott SR, Nariculam J, Box G, Munson P, Constantinou J, Feneley MR, Klocker H, Eccles SA, Negishi M, Freeman A, Masters JR, Williamson M. 2007. Plexin-B1 mutations in prostate cancer. Proc Natl Acad Sci U S A 104:19040-19045.